STRUCTURAL PROPERTIES OF PHYCOERYTHRIN FROM DULSE PALMARIA PALMATA

YOSHIKATSU MIYABE [1], TOMOE FURUTA [1], TOMOYUKI TAKEDA [1], GAKU KANNO [1], TAKESHI SHIMIZU [2], YOSHIKAZU TANAKA [3, 4], ZUOQI GAI [3], HAJIME YASUI [5] and HIDEKI KISHIMURA [6, 7]

[1] Chair of Marine Chemical Resource Development, Graduate School of Fisheries Sciences, Hokkaido University, Hakodate, Hokkaido 041-8611, Japan

[2] Department of Research and Development, Hokkaido Industrial Technology Center, Hakodate, Hokkaido 041-0801, Japan

[3] Laboratory of X-Ray Structural Biology, Faculty of Advanced Life Science, Hokkaido University, Sapporo 060-0810, Japan

[4] Japan Science and Technology Agency, PRESTO, Sapporo 060-0810, Japan

[5] Laboratory of Humans and the Ocean, Faculty of Fisheries Sciences, Hokkaido University, Hakodate, Hokkaido 041-8611, Japan

[6] Laboratory of Marine Chemical Resource Development, Faculty of Fisheries Sciences, Hokkaido University, Hakodate, Hokkaido 041-8611, Japan

[7] Corresponding author.

TEL/FAX: 81-138-40-5519

EMAIL: kishi@fish.hokudai.ac.jp

Short title: Structural properties of dulse phycoerythrin

ABSTRACT

We found that the red alga dulse (*Palmaria palmata*) contains a lot of proteins, which is mainly composed of phycoerythrin (PE), and the protein hydrolysates showed high angiotensin I converting enzyme (ACE) inhibitory activities. Therefore, we investigated the structure of dulse PE to discuss its structure-function relationship. We prepared the chloroplast DNA and analyzed the nucleotide sequences encoding PE by cDNA cloning method. It was clarified that dulse PE has α- and β-subunits and they are composed by 164 amino acids (MW: 17,638) and 177 amino acids (MW: 18,407), respectively. The dulse PE contained conserved cysteine residues for chromophore attachment site. On the alignment of amino acid sequences of dulse PE with those of other red algal PE, the sequence identities were very high (81-92%). In addition, we purified and crystallized the dulse PE, and its crystal structure was determined at 2.09 Å resolution by molecular replacement method. The revealed 3-D structure of dulse PE which forms an (αβ□□hexamer was similar to other red algal PEs. On the other hand, it was clarified that the dulse PE proteins are rich in hydrophobic amino acid residues (51.0%), especially aromatic amino acid and proline residues. The data imply that the high ACE inhibitory activity of dulse protein hydrolysates would be caused by the specific amino acid composition and sequence of dulse PE.

PRACTICAL APPLICATIONS

Dulse is an abundant and underused resource, which contains a lot of phycobiliproteins. Then, the dulse protein hydrolysates strongly inhibited the activity of angiotensin I converting enzyme. Therefore, it has the potential to be an ingredient of functional food.

KEYWORDS: Red alga; Dulse; *Palmaria palmata*; ACE inhibitory activity; phycoerythrin; Primary structure; 3-D structure

INTRODUCTION

In red algae, phycobiliproteins locate as phycobilisomes on the stromal side of thylakoid membranes in a chloroplast and play a role of light capturing on photosynthesis (Apt *et al*. 1995; Sekar and Chandramohan 2008). The prominent classes of red algal phycobiliproteins are phycoerythrin (PE) followed by phycocyanin (PC) and allophycocyanin (APC), and they are divided on their spectral properties (λ-max of PE = 490-570 nm, λ-max of PC = 610-625 nm, λ-max of APC = 650-660 nm) (Sun *et al*. 2009). Phycobiliproteins of red algae commonly contain α- and β-subunits, and each subunit bears covalently binding one or several phycobilin chromophores at the specific cysteine residues (PE: phycoerythrobilin and phycourobilin, PC: phycocyanobilin and phycoerythrobilin, APC: phycocyanobilin) (Apt *et al.* 1995). The above spectroscopic property of each phycobiliprotein is derived from the specific chromophore composition. The α- and β-subunits of phycobiliprotein combine with each other to form an (αβ) heterodimer, and then three (αβ)s form (αβ□□ trimer arranging a symmetry disc (Apt *et al.* 1995). The discs are organized in supramolecular complexes called phycobilisomes. The core of phycobilisomes is composed of APC discs and the rod is composed of PC and PE discs. On the previous proteomic and genomic studies, some marine red algal phycobiliproteins were studied (Roell and Morse 1993; Ducret *et al*. 1994; Hagopian *et al*. 2004; Niu *et al*. 2006; Tajima *et al*. 2012; Wang *et al*. 2013; DePriest *et al*. 2013). However, there is no information about structural properties of dulse phycobiliproteins.

Dulse (*Palmaria palmata*) is a red alga mainly distributed in high-latitude coastal areas, and it is popular in Ireland and Atlantic Canada as a food and a source of minerals. Fitzgerald *et al.* (2012) and Harnedy *et al*. (2015) also reported the dulse protein hydrolysates show the inhibitory effects for renin and dipeptidyl peptidase IV, respectively. In Japan,

dulse is also distributed around the coast of Hokkaido Prefecture and at Pacific coast of Aomori Prefecture. However, dulse is rarely eaten in Japan. In addition, dulse is even removed from Kombu (*Laminaria* sp.) farming areas in Hokkaido, because it inhibits the growth of young Kombu in winter season. Therefore, we have begun exploring the health benefits of dulse to advance its use as a functional food material. In the previous study, we found that dulse contains a lot of proteins, which are mainly composed of PE followed by PC and APC (Furuta *et al*., 2016). Then, the dulse protein hydrolysates strongly inhibited the activity of angiotensin I converting enzyme (ACE). Moreover, it was suggested that the ACE inhibitory peptides are mainly derived from the dulse PE by thermolysin hydrolysis. Therefore, in this study, we investigated the primary and 3-D structures of dulse PE to discuss its structure-function relationship.

MATERIALS AND METHODS

Materials

Dulse (*P. palmata*) was collected in the coast of Usujiri, Hokkaido, Japan in February. A portion of the thalli was steeped into RNAlater solution (Applied Biosystems, CA, USA) and stored at -80 °C until use.

Restriction enzymes, *Hin*d III and *Ssp* I, were purchased from TaKaRa Bio (Shiga, Japan). RNase A was purchased from Nacalai Tesque (Kyoto, Japan). ACE from rabbit lung was purchased from Sigma Chemical Co. (Mo, USA). Hyppuryl-L-histidyl-L-leucine (Hip-His-Leu), thermolysin (EC 3.4.24.27) from *Bucillus thermoproteolyticus*, pepsin (EC 3.4.23.1) from porcine stomach, and trypsin (EC 3.4.21.4) from bovine pancreas were purchased from Wako Pure Chemical (Osaka, Japan). All other regents were purchased from Wako Pure Chemical (Osaka, Japan).

Preparation of dulse protein hydrolysates

The frozen samples were lyophilized and ground into a fine powder by Wonder Blender WB-1 (OSAKA CHEMICAL Co., Osaka, Japan). Proteins were extracted from the powder by adding 20 v/w of distilled water at 4 °C for 7 h. The extracts were centrifuged (H-200, Kokusan, Tokyo, Japan) at 4 °C, 15,000 x *g* for 10 min, and then the supernatants were used as “dulse proteins”. Some of the dulse proteins were hydrolyzed by 1.0 wt% of thermolysin at 70 °C for 3 h, and the reaction was terminated by heat treatment at 100 °C for 5 min. Subsequently, the solution was centrifuged at 4 °C, 15,000 x *g* for 10 min. The supernatants were dried by lyophilization into the “thermolysin hydrolysates”. Other dulse proteins were

adjusted to pH 2.0, and the proteins were digested by 1.0 wt% of pepsin at 37 °C for 3 h. After the reaction, the pepsin digests were adjusted to pH 8.0. Subsequently, the solutions were centrifuged at 4 °C, 15,000 x *g* for 10 min. The supernatants were dried by lyophilization into the "pepsin hydrolysates". Some of the pepsin hydrolysates were digested by 1.0 wt% of trypsin at 37 °C for 3 h. After that, the digested solutions were boiled for 5 min to inactivate the enzymes, and then centrifuged at 4 °C, 15,000 x *g* for 10 min. The supernatants were dried by lyophilization into the "pepsin-trypsin hydrolysates".

ACE Inhibitory Assay

ACE inhibitory assay was carried out according to the method of Cheung and Cushman (1973) with some modifications. Fifteen microliters of sample solution (5.0 mg/mL) was added to 30 □L of ACE (37 U/mL), and the mixture was incubated at 37 °C for 5 min. Thirty microliters of Hip-His-Leu solution (12.5 mM in 0.1 M sodium borate buffer containing 400 mM NaCl at pH 8.3) was added to the mixture. After incubation at 37 °C for 1 h, the reaction was stopped by adding 75 □L of 1.0 M HCl. The mixture was extracted with 450 μL of ethyl acetate. Four hundred microliters of the upper layer was evaporated, and then the hippuric acid was dissolved in 1.5 mL of distilled water. The absorbance at 228 nm of the solution was measured by a spectrophotometer. The inhibition was calculated from the equation [1- (As-Asb) / (Ac-Acb)] x 100, where Ac is the absorbance of the buffer, Acb is the absorbance when the stop solution was added to the buffer before the reaction, As is the absorbance of the sample, and Asb is the absorbance when the stop solution was added to the sample before the reaction.

Isolation of Dulse Chloroplast DNA

Thawed dulse sample was dissected with scissors and 150 mg of it was put into a microcentrifuge tube. The sample was homogenized in 1.5 mL of TRIzol reagent (Invitrogen, CA, USA) using disperser. Then, 300 μL of chloroform was added to the homogenate, and the solution was mixed. The mixture was centrifuged at 4 ^{o}C, 15,000 x *g* for 20 min, and the supernatant was pooled in a micro tube. Next, equal volume of 2-propanol was added in the tube to precipitate chloroplast DNA, and the solution was centrifuged at 4 ^{o}C, 15,000 x *g* for 20 min. The precipitate was dissolved in 100 μL of TE buffer, and the remaining RNA in it was removed by RNase A treatment (10 μg, 37 ^{o}C, 30 min). After the reaction, 200 μL of sterilized ultrapure water and 300 μL of phenol-chloroform-isoamyl alcohol (25:24:1, v/v/v) were added, and the mixed solution was centrifuged at 4 ^{o}C, 15,000 x *g* for 15 min. Following similar treatment with chloroform-isoamyl alcohol (24:1, v/v), chloroplast DNA was collected by ethanol precipitation. The dried precipitate was dissolved in 100 μL of TE buffer.

Degenerate PCR

Forward primer (PE-F1: ATGCT (A/C/G/T) AA (C/T) GC (A/C/G/T) TTTTC (A/C/G/T) (A/C) G) and reverse primer (PE-R1: CC (A/C/G/T) GC (A/G/T) AT (A/C/G/T) CCCCA (C/T) TC (A/G) TC) for degenerate PCR were designed on the basis of well-conserved regions of red algal PE genes (*rpeB* and *rpeA*) (Fig. 1a). TaKaRa EX *Taq* Hot Start Version (TaKaRa Bio, Shiga, Japan) was used on the amplification. The PCR program for TaKaRa EX *Taq* HS was 40 cycles of 98 ^{o}C for 10 sec, 47 ^{o}C for 30 sec, 72 ^{o}C for 2 min, and 10 min at 72 ^{o}C. The PCR products were separated by low melting agarose gel electrophoresis and

were purified from the gel using Wizard SV Gel and PCR Clean-Up System (Promega, WI, USA).

Inverse PCR

The remaining 5'- and 3'-regions of dulse PE genes were determined by inverse PCR method. Dulse chloroplast DNA was digested with restriction enzymes, *Ssp* I and *Hin*d III. The digested DNA fragments were cleaned by Mini Elute Spin Columns (QIAGEN, Dusseldorf, Germany), and ligated with T4 DNA ligase (TaKaRa Bio, Shiga, Japan) at 16 ^{o}C for 18 h. For amplifications, specific forward (PE-IF1: CATTACTGATGGTAACAAACGC, PE-IF2: GAGACGTTGATCATTATATGCG) and reverse (PE-IR1: TCACTGCCACCAACGTAAGC, PE-IR2: CTCCACCTTCTTTTACAACAGC) primers were designed using the sequence data determined by degenerate PCR (Fig. 1b). TaKaRa EX *Taq* Hot Start Version (TaKaRa Bio, Shiga, Japan) was used on the amplification, and the PCR program was 40 cycles of 98 ^{o}C for 10 sec, 50 ^{o}C for 30 sec, 72 ^{o}C for 2 min, and 10 min at 72 ^{o}C.

Cloning and Sequencing

PCR products were subcloned to pDrive Cloning Vector using QIAGEN PCR Cloning Kit (QIAGEN, Dusseldorf, Germany) for sequencing. The nucleotide sequences of cDNAs were determined with BigDye Terminator v3.1 Cycle Sequencing Kit (Applied Biosystems, CA, USA) using ABI PRISM 310 Genetic Analyzer (Applied Biosystems, CA, USA). Nucleotide and deduced amino acid sequences of dulse PE gene were aligned using CLUSTAL W program (Thompson, *et al*. 1994). Molecular weight and isoelectric point of dulse PE were calculated from deduced amino acid sequences by using Compute pI/Mw tool

190 (Bjellqvist *et al*. 1993; Bjellqvist *et al*. 1994; Hoogland *et al*. 2000).

191

192 Crystallization, X-ray diffraction data collection, and structure determination

193

194 Frozen dulse samples (-30 ^{o}C) were taken into a flask, and 4 volumes (v/w) of distilled water
195 was added in it. The dulse phycobiliproteins were extracted at 4 ^{o}C for 12 h, and the extracts
196 were filtered. Then, the filtrates were centrifuged at 4 ^{o}C, 15,000 x *g* for 15 min. The
197 extracted dulse proteins were dialyzed against distilled water at 4 ^{o}C for 24 h. The dulse PE
198 was purified from the protein extracts by a preparative electrofocusing using Rotofor system
199 (Bio-Rad, CA, USA) (Fig. 4a and 4b). Crystallization was carried out by hanging-drop
200 vapor diffusion method. Crystals of dulse PE were grown from a buffer containing 0.1 M
201 sodium acetate (pH 4.8) and 12% PEG4000 (Fig. 4b). X-ray diffraction dataset of dulse PE
202 was collected on the beamline BL17A at Photon Factory (Tsukuba, Japan) under cryogenic
203 condition (100 K). Crystals were mounted on the X-ray diffractometer after soaked into a
204 crystallization buffer containing 20% PEG400 as a cryoprotectant. The diffraction data were
205 indexed, integrated, scaled, and merged using the XDS program (Kabsch 2010). The data
206 statistics are shown in Table 1. Crystal structures were determined by the molecular
207 replacement method with the program MOLREP (Vagin and Teplyakov 1997) using the
208 structure of PE from *Polysiphonia urceolata* (PDB ID 1LIA) as a search model. To monitor
209 the refinement, a random 5% subset was set aside for the calculation of the R_{free} factor.
210 Structure refinement was carried out with phenix.refine (Adams *et al*. 2010). The
211 stereochemical quality of the structure was analyzed with the program MOLPROBITY (Chen
212 *et al*. 2010). The refinement statistics are summarized in Table 1. The atomic coordinates
213 of dulse PE has been deposited in the Protein Data Bank, www.pdb.org (PDB ID code 5B13).

RESULTS AND DISCUSSION

Inhibition of ACE activity of dulse protein hydrolysates

In the previous study, we found that dulse contains a lot of proteins, which are mainly composed of PE (Furuta *et al*. 2016). The extracted dulse proteins showed slight ACE inhibitory activity, but the activity was extremely enhanced by thermolysin hydrolysis. In addition, nine ACE inhibitory peptides (YRD, AGGEY, VYRT, VDHY, IKGHY, LKNPG, LDY, LRY, FEQDWAS) were isolated from the hydrolysates by reversed-phase high-performance liquid chromatography (HPLC), and the sequences of YRD, AGGEY, VYRT, VDHY, LKNPG, LDY and LRY were detected in the primary structures of PE α- and β-subunits (Furuta *et al*. 2016). From these results, it was suggested that the ACE inhibitory peptides are mainly derived from the dulse PE by thermolysin hydrolysis. Therefore, in this study, we prepared the dulse protein hydrolysates by thermolysin, pepsin, and pepsin-trypsin digestion, and we compared with their ACE inhibitory activity. As shown in Fig. 2, the thermolysin hydrolysates inhibited 88% of ACE activity, and pepsin and pepsin-trypsin hydrolysates also suppressed 72% and 75% of them, respectively. We calculated the peptide sequences derived from the deduced amino acid sequences of dulse PE α- and β- subunits by using PEPTIDEMASS (Wilkins *et al.* 1997). As a result, it was predicted that 76 peptides (α-subunit: 38 peptides, av. length=3, av. mass=346; β- subunit: 38 peptides, av. length=4, av. mass=396) are derived from dulse PE α- and β- subunits by pepsin-trypsin hydrolysis. From the result, ACE inhibitory peptides are also produced from dulse proteins, especially PE, by proteolytic hydrolysis in our digestive tract. In future, we would like to analyze the structural properties of ACE inhibitory peptides in the pepsin-trypsin hydrolysates to compare with those of thermolysin hydrolysates.

239 Then, in the next stage, we investigated the primary and 3-D structures of dulse PE
240 to discuss its structure-function relationship.
241
242 Nucleotide sequences of dulse phycoerythrin genes
243
244 In this study, we obtained 1,560 bp of nucleotide sequences on the analysis of the dulse PE
245 gene, and the gene structure encoding dulse PE (*rpeA* and *rpeB*, GenBank accession number
246 AB625450) (Fig. 3) was clarified. This is the first report for the PE gene of Palmariales.
247 As shown in Fig. 3, the dulse PE gene was constituted of α- and β-subunit genes and
248 A/T-rich spacer. AT contents of the spacer in dulse PE gene were 79% (60 bp/76 bp).
249 Bernard *et al*. (1992) reported that *rpeB* gene of *Rhodella violacea* is split by intervening
250 sequence and the sequence has a feature of group II intron that is typical in eukaryotic
251 organisms, however the dulse PE gene has no introns. The dulse *rpeB* was present in prior
252 to the *rpeA* (Fig. 3). The positions of *rpeA* and *rpeB* were the same as those of other red
253 algae, for example *Gracilaria tenuistipitata* (Hagopian *et al*. 2004), *Chondrus crispus*
254 (GenBank accession number HF562234), *Pyropia yezoensis* (Wang *et al*. 2013), *P.*
255 *haitanensis* (Wang *et al*. 2013) and *P. purpurea* (GenBank accession number U38804). The
256 nucleotide sequences of dulse PE gene also showed considerably high identities (about 80%)
257 with those of other red algae (Table 2). The GC contents in dulse PE gene were about 40%
258 (*rpeA*: 40.2%, *rpeB*: 40.5%), and these numerical values showed very high similarity to those
259 of *P. yezoensis* (*rpeA*: 42.6%, *rpeB*: 40.6%), *P. haitanensis* (*rpeA*: 41.2%, *rpeB*: 41.4%) and *P.*
260 *purpurea* (*rpeA*: 41.8%, *rpeB*: 42.0%), whereas it was a little higher than those of *G.*
261 *tenuistipitata* (*rpeA*: 37.0%, *rpeB*: 38.8%) and *C. crispus* (*rpeA*: 37.2%, *rpeB*: 39.1%) (Table
262 2).
263 The consensus sequences at -10 (5'-TATAAT-3') and -35 (5'-TTGACA-3')

promoter elements for RNA polymerase were searched in the dulse PE genes. As a result, putative motifs were found at upstream regions of *rpeB* (-10: TATATT or TGTAAT, -35: TAAACA or GAAACA) (single and double underlines in Fig. 3). We also sought out the Shine-Dalgarno sequence (5'-AGGAGGT-3') acting as a binding site with 16S rRNA, and then the homologous structures were detected in the upstream of each gene (*rpeB*: AGGAGA, *rpeA*: AGGAGA,) (dotted underlines in Fig. 2).

Primary structure of dulse phycoerythrin

The deduced amino acid sequences of dulse PE α- and β-subunits are shown in Fig. 3. The PE α-subunit consists of 164 amino acids (495 bp), and its molecular weight and isoelectric point were calculated at 17,638 and 5.40, respectively. Red algal PE commonly has two kinds of chromophores, phycoerythrobilin and phycourobilin. Generally, red algal PE α-subunit binds to two phycoerythrobilin with two Cys residues (Lundell *et al*. 1984; Ficner *et al*. 1992), and the dulse PE α-subunit also retained Cys residues at the corresponding positions (αCys82 and αCys139 in Fig. 3 and Fig. 4a). The dulse PE β-subunit consists of 177 amino acids (534 bp), and its molecular weight and isoelectric point were calculated at 18,407 and 5.42, respectively. It is already known that one phycourobilin and two phycoerythrobilins bind to four Cys residues in β-subunit apo-protein through thioether linkage (Lundell, *et al*. 1984; Ficner *et al*. 1992). In the dulse PE β-subunit, corresponding Cys residues binding with phycourobilin (βCys50 and βCys61 in Fig. 3 and Fig. 4b) and with phycoerythrobilins (βCys82 and βCys158) were all conserved.

3-D structures of dulse phycoerythrin

289 We purified and crystallized the dulse PE (Fig.5a), and its crystal structure was determined by
290 molecular replacement method (Fig.5b and Table 1). The revealed 3-D structure of purified
291 dulse PE in this study formed an (αβ□□hexamer, which was similar to other red algal PEs
292 (Chang *et al*. 1996; Contreras-Martel *et al*. 2001; Ritter *et al*. 1999). The root mean square
293 deviations (r.m.s.d) with other PEs are as follows, *Polysiphonia urceolata* PE: 0.70 Å,
294 *Griffithsia monilis* PE: 0.55 Å, *Gracilaria chilensis* PE: 0.60 Å. As observed for other
295 homologous phycobiliproteins such as PE, PC and APC, the backbone conformations of α-
296 and β-subunits of dulse PE have nine α-helices (X, Y, A, B, E, F', F, G, and H) as a dominant
297 secondary structure element (Fig. 5b) (Lundell *et al*. 1984; Ficner *et al*. 1992; Liu *et al*. 1999;
298 Jiang *et al*. 2001). Each subunit had a structure quite similar to those of other PEs. The
299 r.m.s.d. was 0.39 Å, 0.33 Å, and 0.37 Å for α-subunit, and 0.56 Å, 0.48Å, and 0.55Å for
300 β-subunit of *P. urceolata* PE, *G. monilis* PE and *G. chilensis* PE, respectively. The electron
301 density clearly showed the presence of chromophores covalently linked to Cys residue
302 through thioether bond. Phycoerythrobilins were linked covalently with each of αCys82,
303 αCys139, βCys82, and βCys158, whereas a phycourobilin was linked doubly to βCys50 and
304 βCys61. The presence of chromophores at these sites is highly conserved among PEs of
305 which structures have been reported (Camara-Artigas *et al*. 2012; Chang *et al*. 1996;
306 Contreras-Martel *et al*. 2001; Lundell *et al*. 1984; Ritter *et al*. 1999). Taken these
307 observations together, we concluded that dulse PE has structural characteristics common to
308 other PEs.
309
310 Structure-function relationship of dulse phycoerythrin
311
312 ACE is a key enzyme in the regulation of peripheral blood pressure catalyzing the production
313 of angiotensin II and the destruction of bradykinin (Cheung *et al*. 1980). The specific

314 inhibitors of the enzyme therefore have been considered with effective antihypertensive drugs.
315 In addition to the drugs, ACE inhibitory peptides from daily food are also useful for
316 maintaining blood pressure at a healthy level. Although the potency of peptide is lower than
317 drug, it does not have side effect (Balti *et al*. 2015). Up to now, many researchers have
318 identified various ACE inhibitory peptides from the enzymatic hydrolysates of food (Amado
319 *et al*. 2014; Ghassem *et al*. 2014; Balti *et al*. 2015; García-Moreno *et al*. 2015). Besides,
320 Cheung *et al*. (1980) obtained the interesting results by using several synthetic peptides for a
321 substrate of ACE, that is to say, the ACE inhibitory activity of peptide is closely related to the
322 C-terminal dipeptide residues in it. Specifically, in case of tryptophan, tyrosine, or proline
323 residue is located at the N-terminal side of dipeptide and aromatic amino acid or proline
324 residue is at the C-terminus, its inhibitory potency is the most. Indeed, it has been well
325 known that the peptides are usually composed of hydrophobic and aromatic amino acids
326 (Amado *et al*. 2014; Ghassem *et al*. 2014; Balti *et al*. 2015; García-Moreno *et al*. 2015).
327 Therefore, we calculated the contents of hydrophobic and aromatic amino acid residues in
328 dulse PE by using the primary structures in this study (Fig. 3). As a result, it was clarified
329 that the dulse PE are rich in hydrophobic amino acids (51.0%), especially the contents of
330 aromatic amino acids and proline (10.0-10.9%) are relatively high. On the other hand,
331 crystal structure analysis clearly showed that dulse PE shares significant similarity in their
332 tertiary structure with other PEs. Therefore, we concluded that the cause of high ACE
333 inhibitory activity of dulse PE hydrolysates would be the specific amino acid compositions
334 and sequences, independent of the tertiary structure.

ACKNOWLEDGMENTS

We thank Dr. Koji Mikami, Faculty of Fisheries Sciences, Hokkaido University, for the technical assistance of inverse PCR. We thank Dr. Hiroki Saeki, Faculty of Fisheries Sciences, Hokkaido University, for the technical assistance of preparative electrofocusing using Rotofor system. We also thank Mr. Yuki Kato, Hokkaido Industrial Technology Center, for the operative support of DNA sequencer.

This work was supported in part by the Regional Innovation Cluster Program (Global Type), Ministry of Education, Culture, Sports, Science and Technology, Japan and the Grant-in-Aid for High Technology Research Program from the Ministry of Education, Culture, Sports, Science, and Technology of Japan. This work was supported in part by Grants-in-Aid for Scientific Research (24000011, 20374225, and 16H00748 to YT) and Platform for Drug Discovery, Informatics, and Structural Life Science from the Ministry of Education, Culture, Sports, Science and Technology, Japan, and JST, PRESTO (YT).

REFERENCES

APT, K.E., COLLIER, J.L. and GROSSMAN, A.R. 1995. Evolution of the phycobiliproteins. J. Mol. Biol. *248*, 79-96.

ADAMS, P.D., AFONINE, P.V., BUNKOCZI, G., CHEN, V.B., DAVIS, I.W., ECHOLS, N., HEADD, J.J., HUNG, L.W., KAPRAL, G.J., GROSSE-KUNSTLEVE, R.W., MCCOY, A.J., MORIARTY, N.W., OEFFNER, R., READ, R.J., RICHARDSON, D.C., RICHARDSON, J.S., TERWILLIGER, T.C. and ZWART, P.H. 2010. PHENIX: a comprehensive Python-based system for macromolecular structuresolution. Acta Crystallogr. *D66*, 213-221.

AMADO, I.R., VAZQUEZ, J.A., GONZALEZ, P., ESTEBAN-FERNANDEZ, D., CARRERA, M. and PINEIRO, C. 2014. Identification of the major ACE-inhibitory peptides produced by enzymatic hydrolysis of a protein concentrate from cuttlefish wastewater. Marine Drugs *12*, 1390-1405.

BERNARD, C., THOMAS, J.C., MAZEL, D., MOUSSEAU, A., CASTETS, A.M., DE MARSAC, N.T. and DUBACQ, J.P. 1992. Characterization of the genes encoding phycoerythrin in the red alga *Rhodella violacea*: evidence for a splitting of the *rpeB* gene by an intron. Proc. Natl. Acad. Sci. U.S.A. *89*, 9564-9568.

BJELLQVIST, B., HUGHES, G., PASQUALI, C., PAQUET, N., RAVIER, F., SANCHEZ, J.-C., FRUTIGER, S. and HOCHSTRASSER, D.F. 1993. The focusing positions of polypeptides in immobilized pH gradients can be predicted from their amino acid sequences. Electrophoresis *14*, 1023–1031.

BJELLQVIST, B., BASSE, B., OLSEN, E. and CELIS, J.E. 1994. Reference points for comparisons of two-dimensional maps of proteins from different human cell types defined in a pH scale where isoelectric points correlate with polypeptide compositions.

Electrophoresis *15*, 529–539.

BALTI, R., BOUGATEF, A., SILA, A., GUILLOCHON, D., DHULSTER, P. and NEDJAR-ARROUME, N. 2015. Nine novel angiotensin I-converting enzyme (ACE) inhibitory peptides from cuttlefish (*Sepia officinalis*) muscle protein hydrolysates and antihypertensive effect of the potent active peptide in spontaneously hypertensive rats. Food Chem. *170*, 519-525.

CHEUNG, H.S. and CUSHMAN, D.W. 1973. Inhibition of homogeneous angiotensin-converting enzyme of rabbit lung by synthetic venom peptides of *Bothrops jararaca*. Biochim. Biophys. Acta *293*, 451-463.

CHEUNG, H.S., WANG, F.L., ONDETTI, M.A., SABO, E.F. and CUSHMAN, D.W. 1980. Binding of peptide substrates and inhibitors of angiotensin-converting enzyme: importance of the COOH-terminal dipeptide sequence. J. Biol. Chem. *25*, 401-407.

CHANG, W.R., JIANG, T., WAN, Z.L., ZHANG, J.P., YANG, Z.X. and LIANG, D.C. 1996. Crystal structure of R-phycoerythrin from Polysiphonia urceolata at 2.8 Å resolution. J. Mol. Biol. *262*, 721-31.

CONTRERAS-MARTEL, C., MARTINEZ-OYANEDEL, J., BUNSTER, M., LEGRAND, P., PIRAS, C., VERNEDE, X. and FONTECILLA-CAMPS, J.C. 2001. Crystallization and 2.2 Å resolution structure of R-phycoerythrin from Gracilaria chilensis: a case of perfect hemihedral twinning. Acta Crystallogr. *D57*, 52-60.

CHEN, V.B., ARENDALL 3rd. W.B., HEADD, J.J., KEEDY, D.A., IMMORMINO, R.M., KAPRAL, G.J., MURRAY, L.W., RICHARDSON, J.S. and RICHARDSON, D.C. 2010. MolProbity: all-atomstructure validation for macromolecular crystallography. Acta Crystallogr. *D66*, 12-21.

CAMARA-ARTIGAS, A., BACARIZO, J., ANDUJAR-SANCHEZ, M., ORTIZ-SALMERON, E., MESA-VALLE, C., CUADRI, C., … and ALLEN, J.P. 2012. pH-dependent structural conformations of B-phycoerythrin from Porphyridium cruentum. FEBS J. *279*, 3680-91.

DUCRET, A., SIDLER, W., FRANK, G. and ZUBER, H. 1994. The complete amino acid sequence of R-phycocyanin-I α and β subunits from the red alga *Porphyridium cruentum*: structural and phylogenetic relationship of the phycocyanins within the phycobiliprotein families. Eur. J. Biochem. *221*, 563-580.

DEPRIEST, M.S., BHATTACHARYA, D. and LOPEZ-BAUTISTA, J.M. 2013. The plastid genome of the red macroalga *Grateloupia taiwanensis* (Halymeniaceae). PLoS One, *8*, e68246.

FICNER, R., LOBECK, K., SCHMIDT, G. and HUBER, R. 1992. Isolation, crystallization, structure analysis and refinement of B-phycoerythrin from the red alga *Porphyridium sordidum* at 2.2 Å resolution. J. Mol. Biol. *228*, 935-950.

FITZGERALD, C., MORA-SOLER, L., GALLAGHER, E., O'CONNOR, P., PRIETO, J., SOLER-VILA, A. and HAYES, M. 2012. Isolation and characterization of bioactive pro-peptides with *in vitro* renin inhibitory activities from the macroalga *Palmaria palmata*. J. Agric. Food Chem. *60*, 7421-7427.

FURUTA, T., MIYABE, Y., YASUI, H., KINOSHITA, Y. and KISHIMURA, H. 2016. Angiotensin I converting enzyme inhibitory peptides derived from phycobiliproteins of dulse *Palmaria palmata*. Marine Drugs , *14*, 32; doi:10.3390/md14020032.

GHASSEM, M., BABJI, A.S., SAID, M., MAHMOODANI, F. and AEIHARA, K. 2014. Angiotensin I-converting enzyme inhibitory peptides from snakehead fish sarcoplasmic protein hydrolysate. J. Food Biochem. *38*, 140-149.

422 GARCIA-MORENO, P.J., ESPEJO-CARPIO, F.J., GUADIX, A. and GUADIX, E.M. 2015.
423 Production and identification of angiotensin I-converting enzyme (ACE) inhibitory
424 peptides from Mediterranean fish discards. J. Func. Foods *18*, 95-105.
425 HOOGLAND, C., SANCHEZ, J.-C., TONELLA, L., BINZ, P.-A., BAIROCH, A.,
426 HOCHSTRASSER, D.F. and APPEL, R.D. 2000. The 1999 SWISS-2DPAGE database
427 update. Nucleic Acids Res. *28*, 286–288.
428 HAGOPIAN, J.C., REIS, M., KITAJIMA, J.P., BHATTACHARYA, D. and DE OLIVEIRA,
429 M.C. 2004. Comparative analysis of the complete plastid genome sequence of the red alga
430 *Gracilaria tenuistipitata* var. *liui* provides insights into the evolution of rhodoplasts and
431 their relationship to other plastids. J. Mol. Evol. *59*, 464-477.
432 HARNEDY, P.A., O'KEEFFE, M.B. and FITZGERALD, R.J. 2015. Purification and
433 identification of dipeptidyl peptidase (DPP) IV inhibitory peptides from the macroalga
434 *Palmaria palmata*. Food Chem. *172*, 400-406.
435 JIANG, T., ZHANG, J.P., CHANG, W.R. and LIANG, D.C. 2001. Crystal structure of
436 R-phycocyanin and possible energy transfer pathway in the phycobilisomes. Biophys. J.
437 *81*, 1171-1179.
438 KABSCH, W. 2010. Xds. Acta Crystallogr. *D66*, 125-132.
439 LUNDELL, D.J., GLAZER, A.N, DELANGE, R.J. and BROWN, D.M. 1984. Bilin
440 attachment sites in the α- and β-subunits of B-phycoerythrin: amino acid sequence
441 studies. J. Biol. Chem. *259*, 5472-5480.
442 LIU, J.Y., JIANG, T., ZHANG, J.P. and LIANG, D.C. 1999. Crystal structure of
443 allophycocyanin from red algae *Porphyra yezoensis* at 2.2- Å resolution. J. Biol. Chem.
444 *274*, 16945-16952.
445 NIU, J.F., WANG, G.C. and TSENG, C.K. 2006. Method for large-scale isolation and
446 purification of R-phycoerythrin from red alga *Polysiphonia urceolata* Grev. Protein Expr.

Purif. *49*, 23-33.

ROELL, M.K. and MORSE, D.E. 1993. Organization, expression and nucleotide sequence of the operon encoding R-phycoerythrin [illegible] subunits from the red *boldii*. Plant Mol. Biol. *21*, 47-58.

RITTER, S., HILLER, R. G., WRENCH, P. M., WELTE, W. and DIEDERICHS, K. 1999. Crystal structure of a phycourobilin-containing phycoerythrin at 1.90- Å resolution. J. Struc. Biol. *126*, 86–97.

SEKAR, S. and CHANDRAMOHAN, M. 2008. Phycobiliproteins as a commodity: trends in applied research, patents and commercialization. J. Appl. Phycol. *20*, 113-136.

SUN, L., WANG, S., GONG, X., ZHAO, M., FU, X. and WANG, L. 2009. Isolation, purification and characteristics of R-phycoerythrin from a marine macroalga *Heterosiphonia japonica*. Protein Expr. Purif. *64*, 146-154.

THOMPSON, J.D., HIGGINS, D.G. and GIBSON, T.J. 1994. CLUSTAL W: improving the sensitivity of progressive multiple sequence alignment through sequence weighting, positions-specific gap penalties and weight matrix choice. Nucleic Acids Res. *22*, 4673-4680.

TAJIMA, N., SATO, S., MARUYAMA, F., KUROKAWA, K., OHTA, H., TABATA, S., SEKINE, K., MORIYAMA, T. and SATO, N. 2012. Analysis of the complete chloroplast genome of the unicellular red alga *Porphyridium purpureum*. Photosynthetic Res. *22*, 156-159.

VAGIN, A. and TEPLYAKOV, A. 1997. MOLREP: an automated program for molecular replacement. J. Appl. Crystallogr. *30*, 1022-1025.

WILKINS M.R., LINDSKOG I., GASTEIGER E., BAIROCH A., SANCHEZ J.C., HOCHSTRASSER D.F. and APPEL R.D. 1997. Detailed peptide characterization using

PEPTIDEMASS - a World-Wide-Web-accessible tool. Electrophoresis, *18*, 403-408.

WANG, L., MAO, Y.X., KONG, F.N., LI, G.Y., MA, F., ZHANG, B.L., SUN, P.P., BI, G.Q., ZHANG, F.F., XUE, H.F. and CAO, M. 2013. Complete sequence and analysis of plastid genomes of two economically important red algae: *Pyropia haitanensis* and *Pyropia yezoensis*. PLoS One, *8*, e65902.

(Captions to figures)

FIG. 1. GENERAL STRUCTURES OF RED ALGAL PHYCOERYTHRIN GENES AND POSITIONS OF PRIMERS USED IN DEGENERATE AND INVERSE PCRS.

a: Positions of primers used in degenerate PCR.

b: Positions of primers used in inverse PCR.

PE represent phycoerythrin. Sequences of each primer are shown in the text. Restriction sites are expressed as *Ssp* I, *Hin*d III.

FIG. 2. ACE INHIBITORY ACTIVITIES BY DULSE PROTEIN HYDROLYSATES.

1: ACE inhibitory activity with thermolysin hydrolysates.

2: ACE inhibitory activity with pepsin hydrolysates.

3: ACE inhibitory activity with pepsin-trypsin hydrolysates.

FIG. 3. NUCLEOTIDE AND DEDUCED AMINO ACID SEQUENCES OF DULSE PHYCOERYTHRIN GENE.

Asterisks show stop codon. Single and double underlines express putative -10 and -35 consensus sequences, respectively. Dotted underline is putative RNA polymerase-binding motif.

FIG. 4. ALIGNMENT OF AMINO ACID SEQUENCES OF RED ALGAL PHYCOERYTHRINS.

a: PEα; Phycoerythrin α-subunit.

b: PEβ; Phycoerythrin β-subunit.

Asterisks show characteristic amino acid residues in the molecule. *P. palmata* (GenBank accession number: AB625450, in this study); *G. tenuistipitata* (AY673996), *C.*

crispus (HF562234), *P. yezoensis* (D89878), *P. haitanensis* (DQ449070), *P. purpurea* (U38804).

FIG. 5. DULSE PHYCOERYTHRIN CRYSTAL AND 3-D STRUCTURE OF DULSE PHYCOERYTHRIN.

a: Crystallization of purified dulse phycoerythrin.

Purified PE: purified dulse phycoerythrin. PE crystal: dulse phycoerythrin crystal.

b: 3-D structure of dulse phycoerythrin.

PE (αβ□□ □□□□ mer: Ribbon representation of dulse phycoerythrin (αβ□□□□□□ mer. The α- and β-subunits are colored red and blue, respectively. For clarity, one subunit of α- and β-subunit is colored orange and green, respectively. The bound CYC and PUB are also shown as yellow and green sticks, respectively. PEα: Ribbon representation of dulse phycoerythrin α-subunit. The model is colored according to the sequence from blue at the N-terminus to red at the C-terminus. Bound CYC chromophores are shown as yellow sticks. The cysteine resides linked with the chromophres are also shown. PEβ: Ribbon representation of dulse phycoerythrin β-subunit colored according to the sequence from blue at the N-terminus to red at the C-terminus. Bound CYC and PUB chromophores are shown as yellow and green sticks.

TABLE 1 DATA COLLECTION AND REFINEMENT STATISTICS

Data collection	
Beamline	Photon Factory BL17A
Space group	*C*2
Cell dimensions	
a, b, c (Å)	187.5, 111.9, 112.7
α, β, γ (°)	90.0, 91.9, 90.0
Wavelength (Å)	0.98
Resolution (Å) [a]	50–2.09 (2.22–2.09)
No. of total/unique reflections	519,606/135,827 (81,130/21,390)
R_{sym} (%) [a, b]	11.6 (69.9)
Completeness (%) [a]	99.5 (97.6)
Multiplicity [a]	3.8 (3.8)
Average $I/\sigma(I)$ [a]	11.21 (2.13)
Refinement	
Resolution (Å)	50–2.09
R_{work}/R_{free}	0.198/0.237
No. of atoms	
Protein	15,114
Ligand	1,290
Solvent	1,812
r.m.s.d.	
Bond lengths (Å)	0.003
Bond angles (°)	1.318
Ramachandran plot	
Favored (%)	97.6
Allowed (%)	2.4
Outlier (%)	0

a Values in parentheses correspond to the highest resolution shell.

b $R_{merge} = \Sigma_h \Sigma_i |I_{h,i} - \langle I_h \rangle| / \Sigma_h \Sigma_i |I_{h,i}|$, where $\langle I_h \rangle$ is the mean intensity of a set of equivalent reflections.

TABLE 2. GC CONTENT, NUCLEOTIDE IDENTITY, AND AMINO ACID IDENTITY ON RED ALGAL PHYCOERYTHRINS

Organism		Gene name	GC content (%)	Nucleotide identity to *P.palmata* (%)	Amino acid identity to *P.palmata* (%)	Accession No.
Palmaria palmata	PE	α-subunit	40.2	—	—	AB625450
		β-subnuit	40.5	—	—	
Gracilaria tenuistipitata	PE	α-subunit	37.0	79	87	AY673996
		β-subnuit	38.8	78	81	
Chondrus crispus	PE	α-subunit	37.2	82	85	HF562234
		β-subnuit	39.1	80	85	
Porphyra yezoensis	PE	α-subunit	42.6	82	89	D89878
		β-subnuit	40.6	82	92	
Porphyra haitanensis	PE	α-subunit	41.2	83	90	HM008261
		β-subnuit	41.4	83	92	
Porphyra purpurea	PE	α-subunit	41.8	82	90	NC_000925.1
		β-subnuit	42.0	83	92	

FIG. 1

a: degenerate PCR

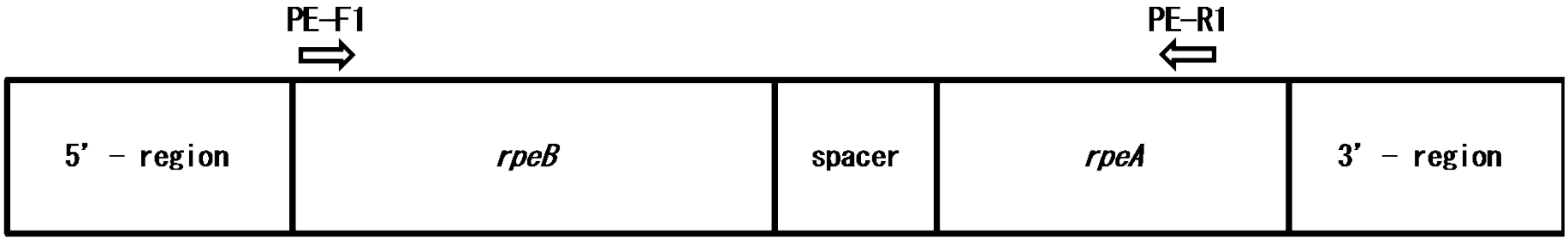

b: invers PCR

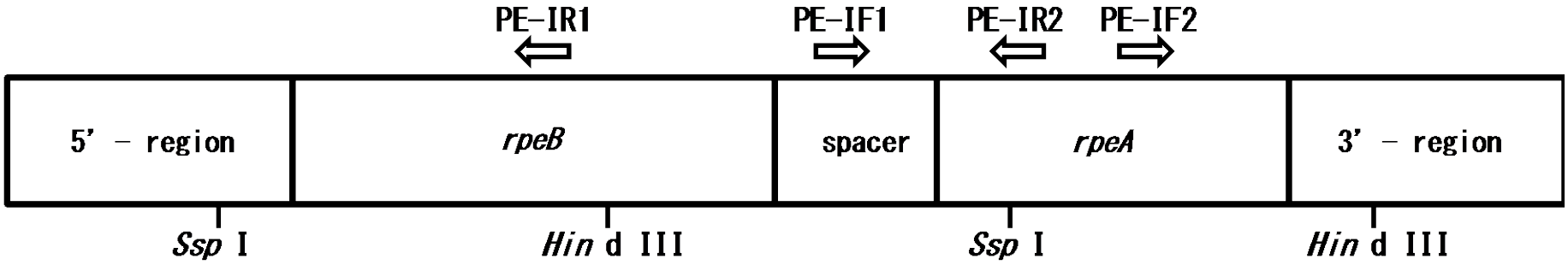

FIG. 2

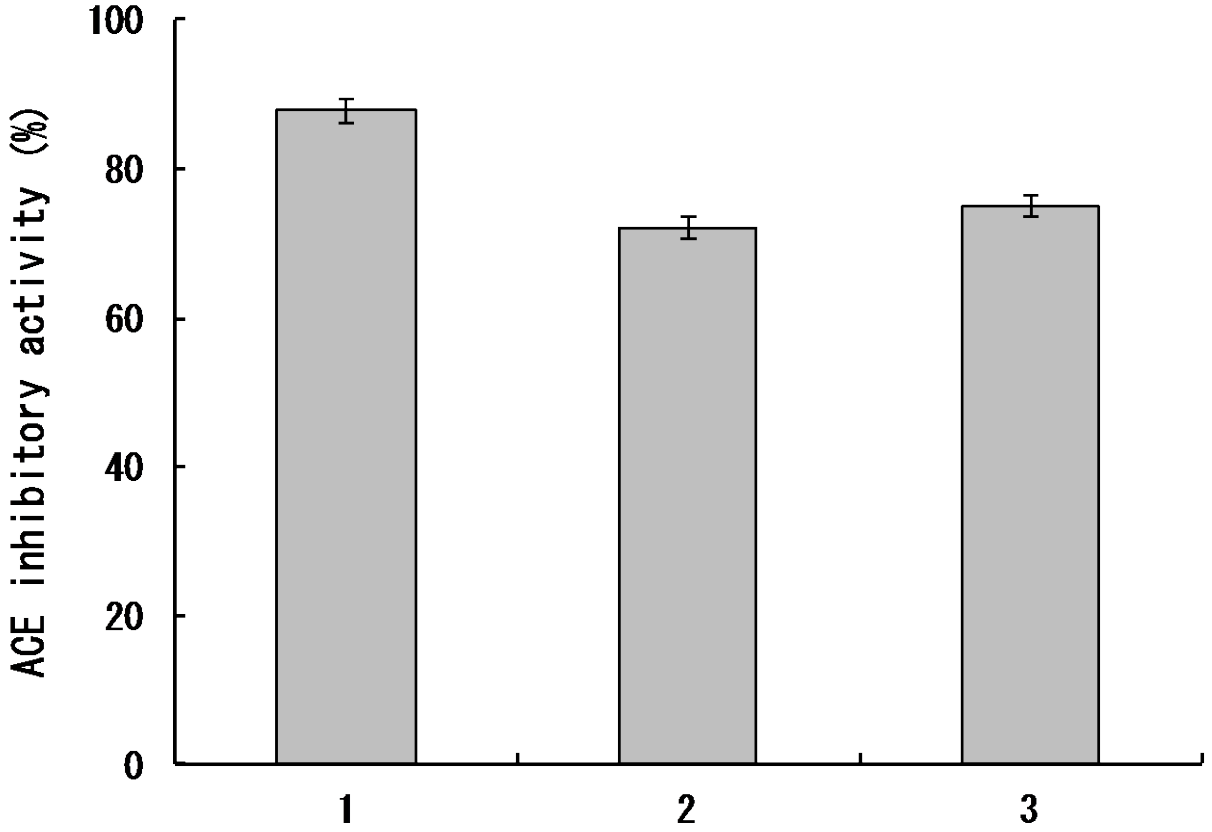

FIG. 3

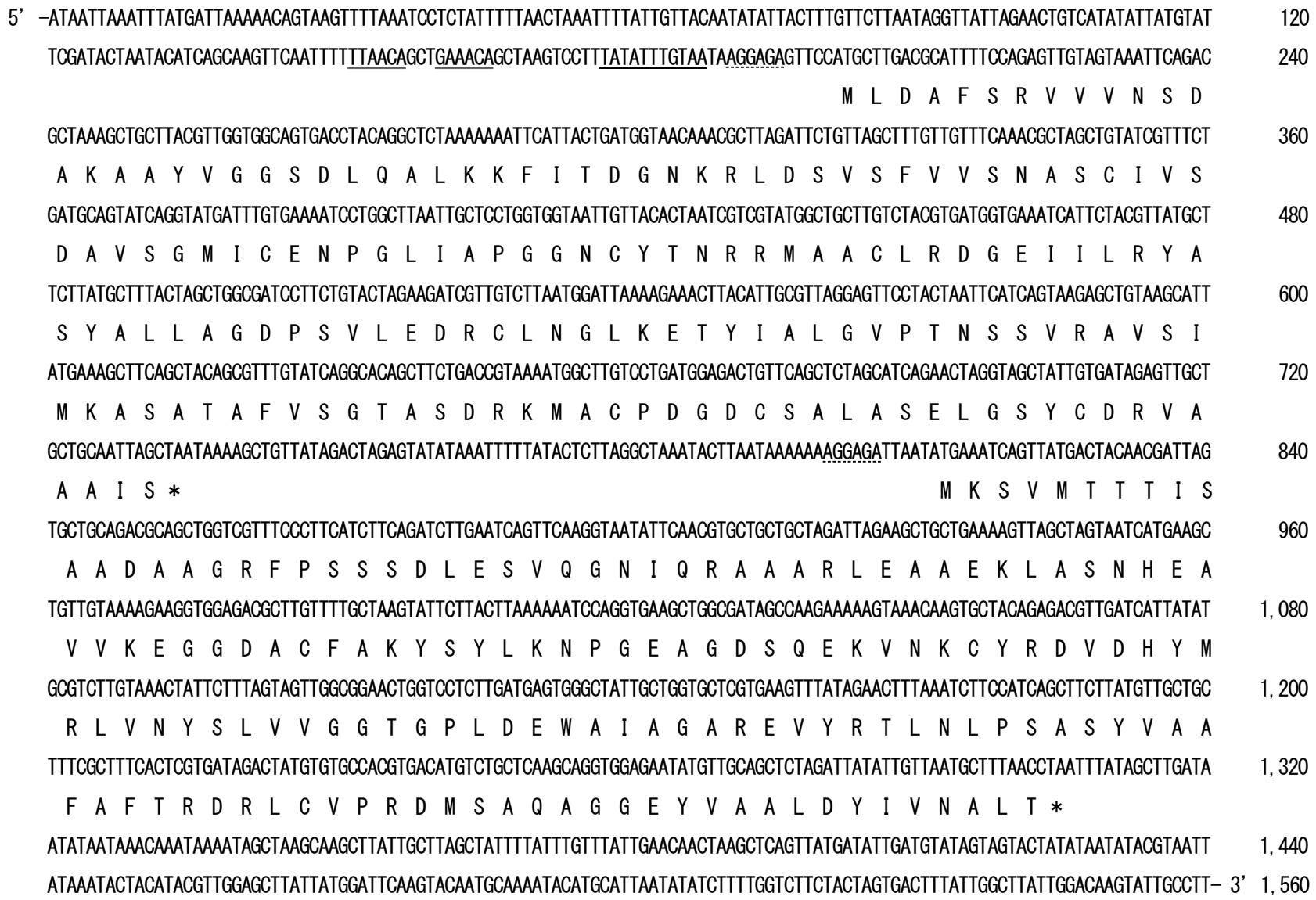
5’ -ATAATTAAATTTATGATTAAAAACAGTAAGTTTTAAATCCTCTATTTTTAACTAAATTTTATTGTTACAATATATTACTTTGTTCTTAATAGGTTATTAGAACTGTCATATATTATGTAT 120
TCGATACTAATACATCAGCAAGTTCAATTTTTTAACAGCTGAAACAGCTAAGTCCTTTATATTTGTAATAAGGAGAGTTCCATGCTTGACGCATTTTCCAGAGTTGTAGTAAATTCAGAC 240
M L D A F S R V V V N S D
GCTAAAGCTGCTTACGTTGGTGGCAGTGACCTACAGGCTCTAAAAAAATTCATTACTGATGGTAACAAACGCTTAGATTCTGTTAGCTTTGTTGTTTCAAACGCTAGCTGTATCGTTTCT 360
A K A A Y V G G S D L Q A L K K F I T D G N K R L D S V S F V V S N A S C I V S
GATGCAGTATCAGGTATGATTTGTGAAAATCCTGGCTTAATTGCTCCTGGTGGTAATTGTTACACTAATCGTCGTATGGCTGCTTGTCTACGTGATGGTGAAATCATTCTACGTTATGCT 480
D A V S G M I C E N P G L I A P G G N C Y T N R R M A A C L R D G E I I L R Y A
TCTTATGCTTTACTAGCTGGCGATCCTTCTGTACTAGAAGATCGTTGTCTTAATGGATTAAAAGAAACTTACATTGCGTTAGGAGTTCCTACTAATTCATCAGTAAGAGCTGTAAGCATT 600
S Y A L L A G D P S V L E D R C L N G L K E T Y I A L G V P T N S S V R A V S I
ATGAAAGCTTCAGCTACAGCGTTTGTATCAGGCACAGCTTCTGACCGTAAAATGGCTTGTCCTGATGGAGACTGTTCAGCTCTAGCATCAGAACTAGGTAGCTATTGTGATAGAGTTGCT 720
M K A S A T A F V S G T A S D R K M A C P D G D C S A L A S E L G S Y C D R V A
GCTGCAATTAGCTAATAAAAGCTGTTATAGACTAGAGTATATAAATTTTTATACTCTTAGGCTAAATACTTAATAAAAAAAGGAGATTAATATGAAATCAGTTATGACTACAACGATTAG 840
A A I S * M K S V M T T T I S
TGCTGCAGACGCAGCTGGTCGTTTCCCTTCATCTTCAGATCTTGAATCAGTTCAAGGTAATATTCAACGTGCTGCTGCTAGATTAGAAGCTGCTGAAAAGTTAGCTAGTAATCATGAAGC 960
A A D A A G R F P S S S D L E S V Q G N I Q R A A A R L E A A E K L A S N H E A
TGTTGTAAAAGAAGGTGGAGACGCTTGTTTTGCTAAGTATTCTTACTTAAAAAATCCAGGTGAAGCTGGCGATAGCCAAGAAAAAGTAAACAAGTGCTACAGAGACGTTGATCATTATAT 1,080
V V K E G G D A C F A K Y S Y L K N P G E A G D S Q E K V N K C Y R D V D H Y M
GCGTCTTGTAAACTATTCTTTAGTAGTTGGCGGAACTGGTCCTCTTGATGAGTGGGCTATTGCTGGTGCTCGTGAAGTTTATAGAACTTTAAATCTTCCATCAGCTTCTTATGTTGCTGC 1,200
R L V N Y S L V V G G T G P L D E W A I A G A R E V Y R T L N L P S A S Y V A A
TTTCGCTTTCACTCGTGATAGACTATGTGTGCCACGTGACATGTCTGCTCAAGCAGGTGGAGAATATGTTGCAGCTCTAGATTATATTGTTAATGCTTTAACCTAATTTATAGCTTGATA 1,320
F A F T R D R L C V P R D M S A Q A G G E Y V A A L D Y I V N A L T *
ATATAATAAACAAATAAAATAGCTAAGCAAGCTTATTGCTTAGCTATTTTATTTGTTTATTGAACAACTAAGCTCAGTTATGATATTGATGTATAGTAGTACTATATAATATACGTAATT 1,440
ATAAATACTACATACGTTGGAGCTTATTATGGATTCAAGTACAATGCAAAATACATGCATTAATATATCTTTTGGTCTTCTACTAGTGACTTTATTGGCTTATTGGACAAGTATTGCCTT- 3’ 1,560

FIG. 4a

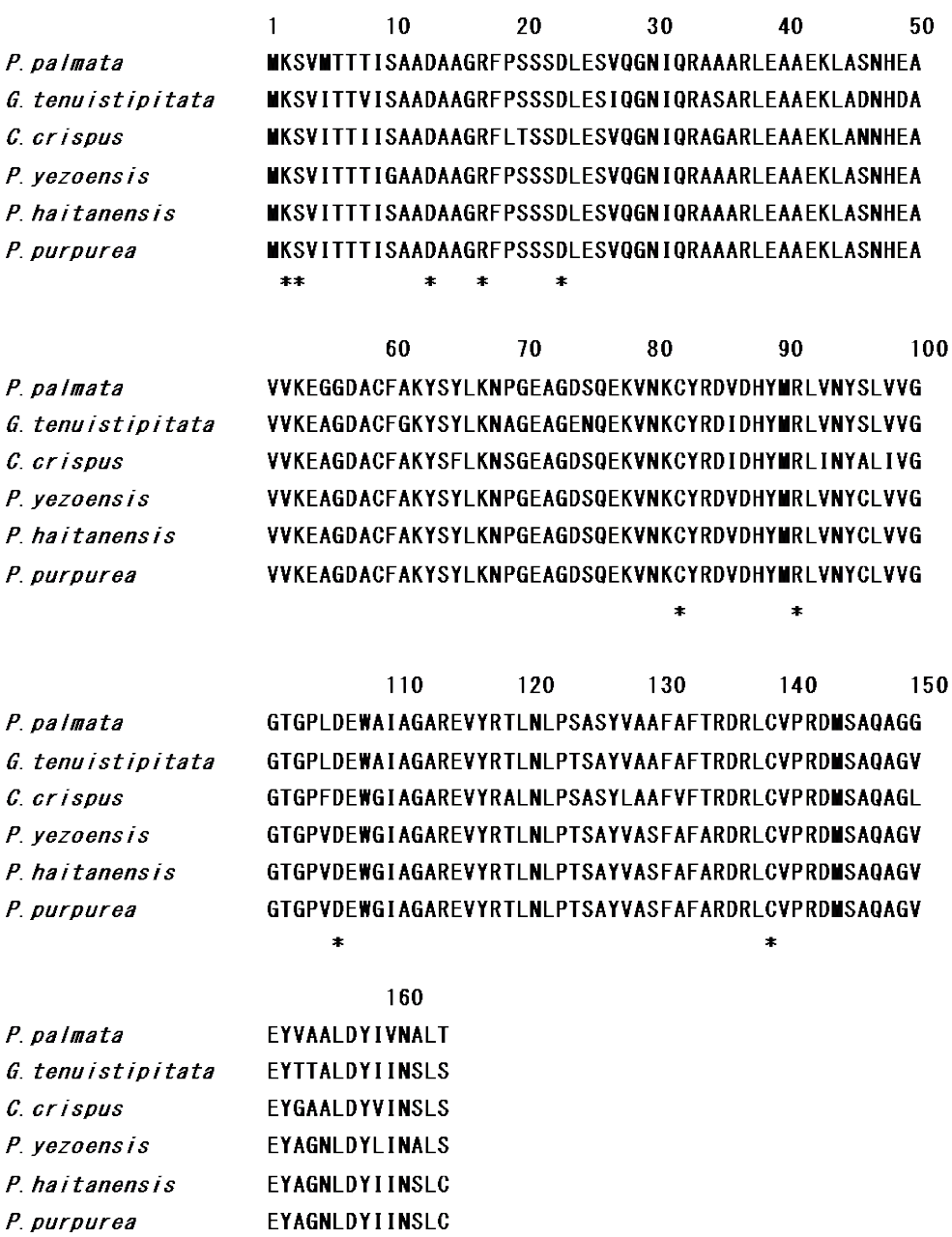
a: PEα
1 10 20 30 40 50
P. palmata MKSVMTTTISAADAAGRFPSSSDLESVQGNIQRAAARLEAAEKLASNHEA
G. tenuistipitata MKSVITTVISAADAAGRFPSSSDLESIQGNIQRASARLEAAEKLADNHDA
C. crispus MKSVITTIISAADAAGRFLTSSDLESVQGNIQRAGARLEAAEKLANNHEA
P. yezoensis MKSVITTTIGAADAAGRFPSSSDLESVQGNIQRAAARLEAAEKLASNHEA
P. haitanensis MKSVITTTISAADAAGRFPSSSDLESVQGNIQRAAARLEAAEKLASNHEA
P. purpurea MKSVITTTISAADAAGRFPSSSDLESVQGNIQRAAARLEAAEKLASNHEA
60 70 80 90 100
P. palmata VVKEGGDACFAKYSYLKNPGEAGDSQEKVNKCYRDVDHYMRLVNYSLVVG
G. tenuistipitata VVKEAGDACFGKYSYLKNAGEAGENQEKVNKCYRDIDHYMRLVNYSLVVG
C. crispus VVKEAGDACFAKYSFLKNSGEAGDSQEKVNKCYRDIDHYMRLINYALIVG
P. yezoensis VVKEAGDACFAKYSYLKNPGEAGDSQEKVNKCYRDVDHYMRLVNYCLVVG
P. haitanensis VVKEAGDACFAKYSYLKNPGEAGDSQEKVNKCYRDVDHYMRLVNYCLVVG
P. purpurea VVKEAGDACFAKYSYLKNPGEAGDSQEKVNKCYRDVDHYMRLVNYCLVVG
110 120 130 140 150
P. palmata GTGPLDEWAIAGAREVYRTLNLPSASYVAAFAFTRDRLCVPRDMSAQAGG
G. tenuistipitata GTGPLDEWAIAGAREVYRTLNLPTSAYVAAFAFTRDRLCVPRDMSAQAGV
C. crispus GTGPFDEWGIAGAREVYRALNLPSASYLAAFVFTRDRLCVPRDMSAQAGL
P. yezoensis GTGPVDEWGIAGAREVYRTLNLPTSAYVASFAFARDRLCVPRDMSAQAGV
P. haitanensis GTGPVDEWGIAGAREVYRTLNLPTSAYVASFAFARDRLCVPRDMSAQAGV
P. purpurea GTGPVDEWGIAGAREVYRTLNLPTSAYVASFAFARDRLCVPRDMSAQAGV
160
P. palmata EYVAALDYIVNALT
G. tenuistipitata EYTTALDYIINSLS
C. crispus EYGAALDYVINSLS
P. yezoensis EYAGNLDYLINALS
P. haitanensis EYAGNLDYIINSLC
P. purpurea EYAGNLDYIINSLC

FIG. 4b

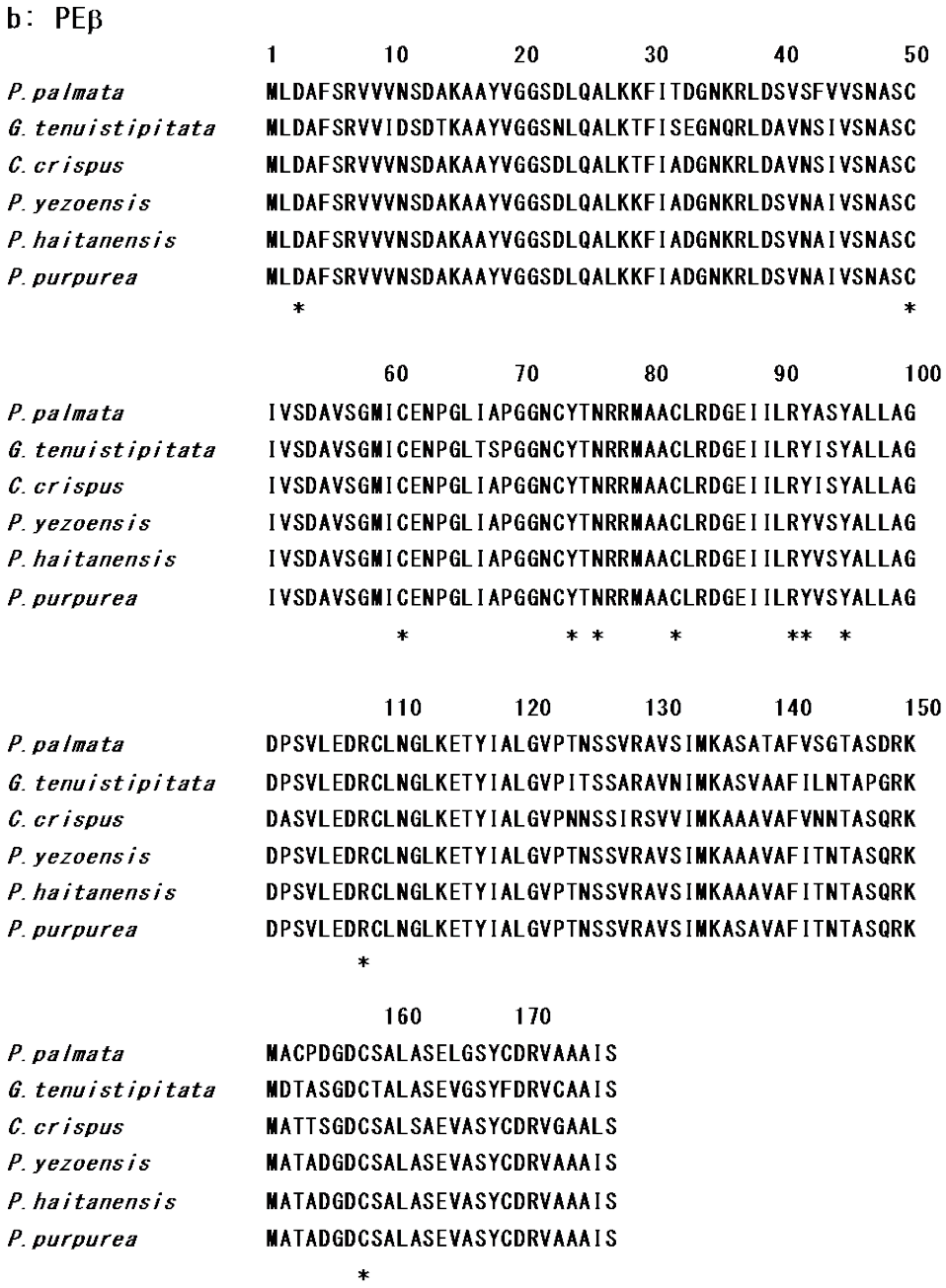
b: PEβ
1 10 20 30 40 50
P. palmata MLDAFSRVVVNSDAKAAYVGGSDLQALKKFITDGNKRLDSVSFVVSNASC
G. tenuistipitata MLDAFSRVVIDSDTKAAYVGGSNLQALKTFISEGNQRLDAVNSIVSNASC
C. crispus MLDAFSRVVVNSDAKAAYVGGSDLQALKTFIADGNKRLDAVNSIVSNASC
P. yezoensis MLDAFSRVVVNSDAKAAYVGGSDLQALKKFIADGNKRLDSVNAIVSNASC
P. haitanensis MLDAFSRVVVNSDAKAAYVGGSDLQALKKFIADGNKRLDSVNAIVSNASC
P. purpurea MLDAFSRVVVNSDAKAAYVGGSDLQALKKFIADGNKRLDSVNAIVSNASC
60 70 80 90 100
P. palmata IVSDAVSGMICENPGLIAPGGNCYTNRRMAACLRDGEIILRYASYALLAG
G. tenuistipitata IVSDAVSGMICENPGLTSPGGNCYTNRRMAACLRDGEIILRYISYALLAG
C. crispus IVSDAVSGMICENPGLIAPGGNCYTNRRMAACLRDGEIILRYISYALLAG
P. yezoensis IVSDAVSGMICENPGLIAPGGNCYTNRRMAACLRDGEIILRYVSYALLAG
P. haitanensis IVSDAVSGMICENPGLIAPGGNCYTNRRMAACLRDGEIILRYVSYALLAG
P. purpurea IVSDAVSGMICENPGLIAPGGNCYTNRRMAACLRDGEIILRYVSYALLAG
110 120 130 140 150
P. palmata DPSVLEDRCLNGLKETYIALGVPTNSSVRAVSIMKASATAFVSGTASDRK
G. tenuistipitata DPSVLEDRCLNGLKETYIALGVPITSSARAVNIMKASVAAFILNTAPGRK
C. crispus DASVLEDRCLNGLKETYIALGVPNNSSIRSVVIMKAAAVAFVNNTASQRK
P. yezoensis DPSVLEDRCLNGLKETYIALGVPTNSSVRAVSIMKAAAVAFITNTASQRK
P. haitanensis DPSVLEDRCLNGLKETYIALGVPTNSSVRAVSIMKAAAVAFITNTASQRK
P. purpurea DPSVLEDRCLNGLKETYIALGVPTNSSVRAVSIMKASAVAFITNTASQRK
160 170
P. palmata MACPDGDCSALASELGSYCDRVAAAIS
G. tenuistipitata MDTASGDCTALASEVGSYFDRVCAAIS
C. crispus MATTSGDCSALSAEVASYCDRVGAALS
P. yezoensis MATADGDCSALASEVASYCDRVAAAIS
P. haitanensis MATADGDCSALASEVASYCDRVAAAIS
P. purpurea MATADGDCSALASEVASYCDRVAAAIS

FIG. 5

a

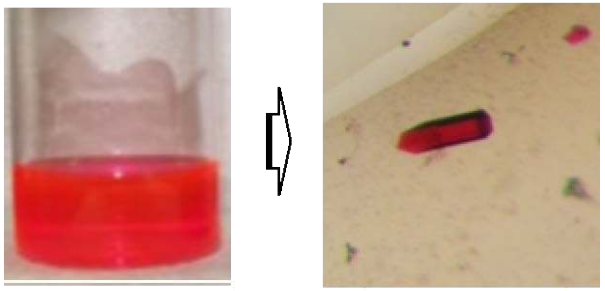
Purified PE
PE crystal

b

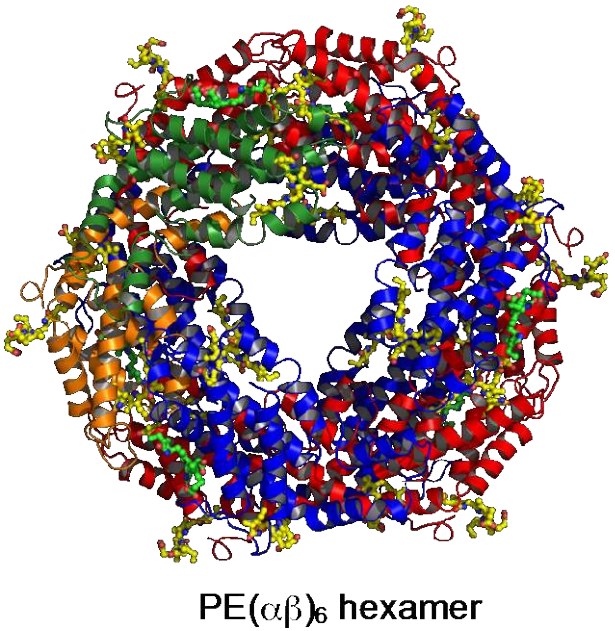
PE(αβ)6 hexamer
αCys82
CYC
CYC
B
F
G
E
F'
H
A
X
αCys139
Y
PEα
βCys61
βCys82
CYC
B
PUB
βCys50
F
E
G
F'
H
A
X
CYC
Y
βCys158
PEβ